



## OPTIMAL DESIGN OF ADVANCED POWER SYSTEMS UNDER UNCERTAINTY

URMILA M. DIWEKAR,<sup>1</sup> EDWARD S. RUBIN<sup>1</sup> and H. CHRISTOPHER FREY<sup>2</sup>

<sup>1</sup>Center for Energy and Environmental Studies, Carnegie Mellon University, Pittsburgh, PA 15213 U.S.A.

<sup>2</sup>Department of Civil Engineering, North Carolina State University, Raleigh, NC 27695 U.S.A.

**Abstract**—Technical and economic uncertainties are not rigorously treated or characterized in most preliminary cost and performance estimates of advanced power system designs. Nor do current design methods rigorously address the issues of design under uncertainty. However, process costs and other important quality measures, such as controllability, safety, and environmental compliance, largely depend on the process synthesis stage. This conceptual design stage involves identifying the basic flowsheet structures from a typically large number of alternatives. This paper describes recent developments in on-going research to develop and demonstrate advanced computer-based methods for dealing with uncertainties that are critical to the design of advanced coal-based power systems. Results are presented illustrating the use of these new modeling tools for the environmental control design of an advanced energy system based on an integrated gasification combined cycle (IGCC) for electric power generation. © 1997 Elsevier Science Ltd.

Process optimization  
control technology

Process synthesis

Uncertainty

Energy systems

Environmental

### INTRODUCTION

Increasing environmental awareness and regulations have placed new requirements on process design for advanced power systems, and increased the need for more sophisticated simulation and design tools to examine pollution prevention options. Conventional process models now in use are largely based on a deterministic framework used for simulation of a specified flowsheet. An important shortcoming of these models is their inability to analyze uncertainties rigorously. Uncertainty analysis capability is especially important in the context of advanced energy systems, since available performance data typically are scant, accurate predictive models do not exist, and many technical as well as economic parameters are not well established.

Though design under uncertainty has received considerable attention in the chemical engineering literature during the past few years, a generalized framework for analyzing uncertainty systematically has only recently been developed around a chemical process simulator [1]. In earlier work, we developed a generalized capability to assign probabilistic values to model input parameters, and to sample these distributions to obtain probabilistic results using Latin Hypercube sampling methods. That capability was built around the ASPEN process simulator [2] developed for the U.S. Department of Energy (USDOE). This stochastic simulation capability has been used successfully to evaluate different configurations of integrated gasification combined cycle (IGCC) systems, an emerging technology for the clean and efficient use of coal for electric power generation. In particular, we have applied probabilistic methods to evaluate the performance, cost, and emissions from IGCC systems, compare alternative systems under conditions of uncertainty, and quantify the benefits from targeted research and development [3-5].

More recently, we have enhanced this framework to include a generalized capability to deal with process synthesis and process optimization. We also have developed a capability to address stochastic optimization and stochastic programming problems, with applications to advanced energy systems. Sequential modular simulators, such as ASPEN and PRO/II, have grown in sophistication over the years and are widely used in the chemical industries to solve complex problems with rigorous process modeling. The USDOE also uses the public version of ASPEN to model a variety of advanced energy systems. Therefore, it was desirable to build the new process synthesis and stochastic optimization capabilities around such simulators. The new capabilities

described in this paper again have been built around the public version of ASPEN. First we describe the methodological basis for these new modeling capabilities, then we present an illustrative case study of their application to the design of environmental controls for an advanced power system.

### METHODOLOGY FOR OPTIMIZATION UNDER UNCERTAINTY

Problems reported in the literature on process design under uncertainty generally are divided into two categories: stochastic optimization, and stochastic programming. Stochastic optimization problems include the "here and now" problems involving expected value minimization, chance constrained optimization, and design for optimal flexibility. These problems all require that at each iteration of the optimization solution method some probabilistic representation of the objective function and constraints are optimized. On the other hand, the "wait and see," "flexibility index," and multiperiod optimization problems involve solving a deterministic optimization problem for each of several "scenarios," so that one gets a probabilistic representation of optimal solutions. These type of problems fall under the category of stochastic programming, namely the effects of uncertainties on optimal design. We describe here the new modeling capability developed for these two general categories of optimization problems under uncertainty.

#### The optimizer

The goal of a classical optimization problem is to determine the values of decision variables  $x$  that maximize some aspect of a deterministic model, represented by the objective function  $Z$ , while ensuring that the model operates within limits established by equality constraints  $h$  and inequality constraints  $g$ . A generalized statement of this problem is given by the following equation:

$$\text{Optimize } Z = z(x) \quad (1)$$

subject to

$$h(x) = 0 \quad (2)$$

$$g(x) \leq 0 \quad (3)$$

where  $x$  is a decision variable vector.

A generalized iterative solution procedure for this traditional deterministic optimization problem is illustrated schematically in Fig. 1. As seen in the figure, the optimizer invokes the model with a set of values for the decision variables  $x$ . The model simulates the flowsheet and calculates values of the objective function and constraints. This information is utilized by the optimizer to calculate a new set of decision variables. This iterative sequence is continued until the optimization criteria are satisfied. This deterministic optimization capability has been implemented in the public version

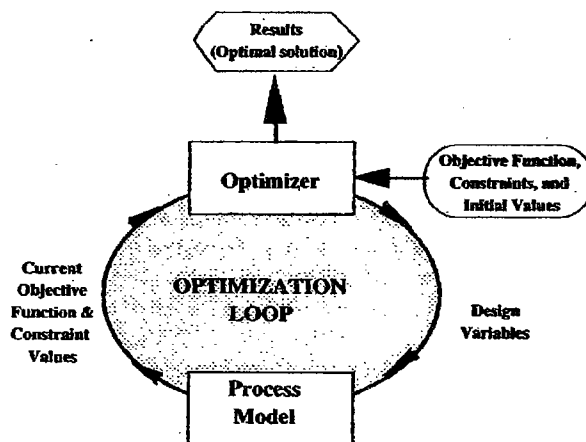


Fig. 1. Schematic of the deterministic optimization framework.

of ASPEN. A new unit operation block (called OPTM) has been developed which solves the nonlinear optimization problem (NLP) described above.

Recent advances in constrained nonlinear optimization techniques provide improved methods for solving large-scale flowsheet problems. The most popular of these methods are generalized reduced gradient (GRG) and successive quadratic programming (SQP), and their variants. Among generalized reduced gradient methods, the most widely used algorithms are GRG2 and MINOS [6].

Most literature on large-scale optimization favors the SQP method because the GRG2 algorithm requires convergence of equality constraints at each iteration. Historically, the GRG strategy has been considered to be the less efficient mode of optimization [7], hence, the GRG2 algorithm is not well-suited for the large-scale optimization problems we are proposing to address. On the other hand, MINOS does not require convergence of equality constraints, and is best suited for optimization problems with linear constraints.

SQP is the most widely used technique for large-scale nonlinear optimization for chemical processes, which typically involve highly nonlinear models. In SQP, at each iteration the problem is approximated as a quadratic program where the objective function is quadratic and the constraints are linear. Similar to linear programming, the special features of a quadratic objective function are exploited to solve the problem more efficiently. The quadratic programming sub-problem is solved for each step to obtain the next trial point. This cycle is repeated until the optimum is reached.

In the ASPEN implementation the NLP optimization block, OPTM, generates decision variable sets using the SQP method [8]. This set is passed to the flowsheet using another new Fortran block (OPTTAIL). After the simulation run, the values of the objective function and constraints are calculated and passed back to the optimization block. The iterations stop when the best improvement to the process for the defined objective function and constraints is found.

As described below, this new NLP optimization capability can be coupled with the stochastic modeling capability developed previously, to solve a broad range of stochastic optimization and stochastic programming problems encountered in practice. The following sections describe this functionality.

#### *Stochastic optimization*

For advanced energy conversion technologies and other processes, the uncertainties associated with process or model input parameters can substantially affect both the performance and cost of those systems. Methods for process design under uncertainty thus become essential. As uncertainty is a broad concept, it is possible, and often useful, to approach it in several different ways. One rather general approach, which has been described earlier and successfully applied to a wide variety of problems, is to assign a probability distribution to the various uncertain input parameters to a model [9]. The generalized stochastic optimization problem, where the decision variables and uncertain parameters are separable, can then be viewed as:

$$\text{Optimize } P1(Z) = P1(z(x, u)) \quad (4)$$

subject to

$$P2(h(x, u)) = 0 \quad (5)$$

$$P3(g(x, u)) \leq 0 \quad (6)$$

where  $u$  is the vector of uncertain parameters and the  $P$  represents the probabilistic functional. For problems where the goal is to minimize an expected value this reduces to:

$$E(F(u)) = \int_0^1 f(u) dp(u). \quad (7)$$

This function can be calculated by sampling the function and calculating the expected value of the samples.

$$E(F(u)) = \frac{\sum_{i=1}^{N_{\text{samp}}} F(u)}{N_{\text{samp}}} \quad (8)$$

On the other hand, for chance constrained optimization problems, where the constraints are represented in terms of a probability of exceeding a certain value, the probabilistic functional is represented by:

$$\text{Optimize } P1(z(x, u)) = E(F(u)) \quad (9)$$

subject to

$$P(h(x, u) > \beta) \leq P_c \quad (10)$$

where equation (10) is a chance constraint.

It is apparent from the above discussion that unlike the deterministic optimization problem, in stochastic optimization one has to consider the probabilistic functional of the objective function and constraints. The generalized treatment of such problems is to use probabilistic or stochastic models instead of a deterministic model inside the optimization loop. Figure 2 represents the generalized stochastic optimization problem solution procedure, where the deterministic model in Fig. 1 is replaced by an iterative stochastic model.

This stochastic optimization capability can also be used to achieve off-line quality control. In off-line quality control, the sensitivity of the design to the sources of variation is reduced at the design stage to make the controller design easier. One such approach based on the concept of Taguchi's parameter design method has been illustrated using the stochastic optimization capability above [9]. This approach involved minimizing the variance of the objective function instead of the expected value.

#### Stochastic programming

In contrast to the stochastic optimization problems, stochastic programming problems concern the effect of uncertainties on optimal design. This involves deterministic decisions at each random stage or random sample, which is the same as solving multiple deterministic optimization problems. This formulation can be represented as:

$$\text{Optimize } Z = z(x, u^*) \quad (11)$$

subject to

$$h(x, u^*) = 0 \quad (12)$$

$$g(x, u^*) \leq 0 \quad (13)$$

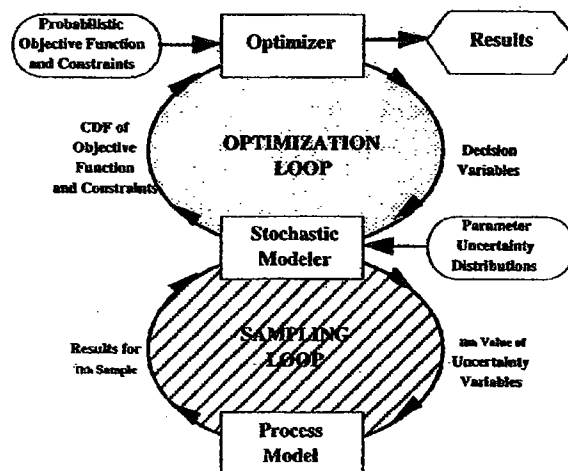


Fig. 2. Schematic of the stochastic optimization framework.

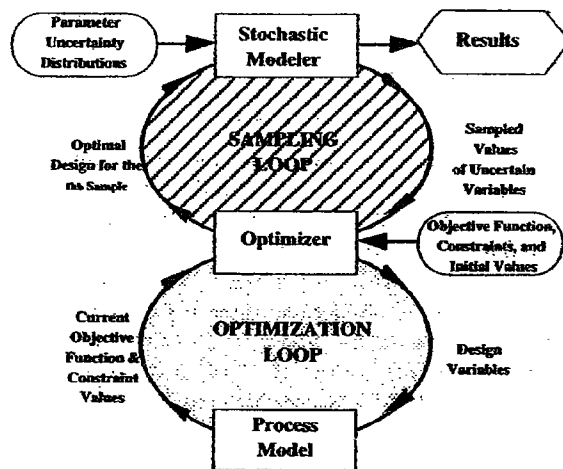


Fig. 3. Schematic of the stochastic programming framework.

where  $u^*$  is the vector of values of uncertain variables corresponding to a particular sample. This optimization procedure is repeated for each sample of uncertain variables  $u$  and a probabilistic representation of outcomes is obtained. Figure 3 represents the generalized solution procedure, where the deterministic problem shown in Fig. 2 forms the inner loop and the stochastic sampling forms the outer loop. This procedure is implemented in the ASPEN simulator by simply interchanging the position of stochastic block, STOCHA, and the optimization block, OPTM. In this way, one can solve almost all the problems in the stochastic optimization/programming literature.

#### METHODOLOGY FOR PROCESS SYNTHESIS

The alternatives for process design and environmental control often are numerous and may involve a very large search space. Selection of the best alternatives can offer the potential for significantly reducing costs and/or improving performance. Therefore, there is a strong need for "systems" research to identify the best ways of configuring advanced energy systems and other complex processes. The current state of process synthesis techniques involves: (a) the heuristic approach which relies on intuition and engineering knowledge; (b) the physical insight approach which is based on exploiting basic physical principles; and (c) the optimization approach which uses mathematical programming techniques. Here we describe a newly developed process synthesizer built around the public version of ASPEN, using the mathematical programming approach [10].

The mathematical programming approach to process synthesis involves:

(a) Formulation of a flowsheet superstructure incorporating all the alternative process configurations.

(b) Modeling the superstructure as a mixed integer nonlinear programming (MINLP) problem of the form:

$$\text{MINLP: } Z = \min_{x, y, \bar{v}} c^T \bar{y} + f(\bar{x}, \bar{v}) \tag{14}$$

subject to

$$h(\bar{x}, \bar{v}) = 0 \tag{15}$$

$$h1(\bar{x}, \bar{v}) = v - z(\bar{x}) = 0$$

$$B^T \bar{y} + g(\bar{x}, \bar{v}) \leq 0$$

$$y \in Y; \quad x \in X$$

where

$$Y = \{y | Ay \leq a, y \in [0, 1]^m\}$$

$$X = \{x | x^L \leq x \leq x^U\}$$

The continuous variables  $x$  represent flows, operating conditions, and design variables. The variables  $v$  are the output variables, which are related to the input variables  $x$  by model equations. For equation-oriented environments, these model equations are embedded in the equality constraints  $h_1(\bar{x}, \bar{v})$ . The binary variables  $y$  denote the presence or absence of specific process units.

(c) Identification of both the optimal configuration and optimal operating process parameters by an algorithm based on an alternating sequence of nonlinear programs (to optimize a given flowsheet) and mixed integer linear programs (to create alternative flowsheets from the model superstructure). This alternating sequence of solution methods is referred to as mixed integer nonlinear programming (MINLP).

#### The MINLP process synthesizer

The newly implemented MINLP process synthesis capability in the public version of ASPEN is based on the mixed integer linear programming (MILP) solver ZOOM [11], and on the nonlinear programming (NLP) solver SCOPT [12]. The method implemented is based on an algorithm called GBD/OA/ER/AP presented by Diwekar *et al.* [10], which involves solving an alternate sequence of MILP and NLP problems. The overall structure of the new synthesis capability is shown in Fig. 4. Optimization of the MINLP process synthesis problem is decomposed into continuous optimization of NLP problems for a fixed choice of binary variables, and discrete optimization through the MILP master problem. The MILP solver (Master) and NLP optimizer have been implemented in ASPEN as unit operation blocks and can be executed easily with the ASPEN process unit blocks.

The process synthesis environment in ASPEN consists of the master block, the NLP optimizer, and the entire superstructure. The initialization of continuous and binary variables is done in the ASPEN input file. At this stage the scheme is translated into an initial flowsheet and subsystems using the decomposition strategy of Kravanja and Grossmann [13]. NLP optimization of the selected flowsheet is the first step in the inner loop. The solution yields the objective function value plus linearization information. This information is passed to the master block which internally modifies the master problem to include the linearization information. The solution of the master problem results in a new flowsheet structure. The iteration stops when there is no improvement in the objective function value.

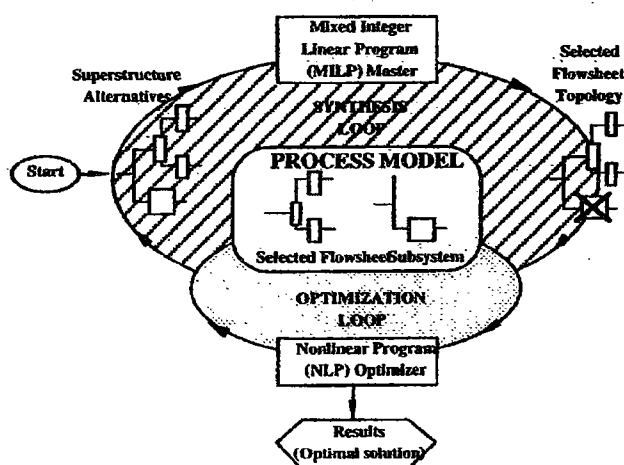


Fig. 4. Schematic of the MINLP synthesizer framework.

### *The implicit constraint problem*

The implementation of this new capability in a sequential modular simulator poses challenging problems which are not encountered in equation-oriented simulators, and new strategies are needed to solve these problems. One such problem associated with the MINLP sequential modular process synthesizer is that of implicit constraints. This problem is encountered because of the "black box" nature of the models in a sequential modular simulator. The ASPEN MINLP environment is based on a two-level optimization algorithm consisting of an upper level MILP master problem and a lower level NLP problem. The MILP master problem predicts new values for binary variables, while the NLP problem provides new values for continuous variables. Since at each stage the MILP master problem obtains linearization information from the NLP optimizer, the MILP master problem represents the linearized NLP problem with non-fixed binary variables. Unlike equation-oriented simulators, in sequential modular simulators most of the nonlinear constraints are not represented explicitly by equations. The linearization information on these constraints, which are essentially black box relations embedded in the simulator environment ( $h1(\bar{x}, \bar{v})$  in equation (15)), therefore, must be passed to the master problem.

In order to circumvent this problem of implicit constraints new decision variables are created. These are equated to the output variables from the flowsheet configurations. This procedure ensures that the original MINLP problem remains the same, while at each stage the MILP master problem receives increased information from the NLP optimizer. Although this procedure assures complete information transfer to the master problem, it also increases the computational load on the NLP optimizer, which is generally the rate-determining step in the MINLP process synthesis. Recently Diwekar and Rubin [14] presented a partitioning strategy which reduces the computational load on the NLP problem, which is crucial for the solution of large-scale synthesis problems.

### *Applications of the new modeling capabilities*

The new capabilities for process synthesis and optimization under uncertainty provide powerful new tools for the design and analysis of advanced energy systems. An application of the new synthesis capability has been described in a recent paper [9], which focuses on choosing a least-cost approach to sulfur removal for an integrated coal gasification combined cycle (IGCC) system with hot gas cleanup and a fluidized bed gasifier. In this paper we show new results that illustrate use of the stochastic optimization and stochastic programming capabilities for the design of an IGCC system.

A 650 MW IGCC system featuring an air-blown dry ash Lurgi gasifier using a high-sulfur Illinois no. 6 coal is analyzed. A hot gas cleanup system is used for high temperature (600°C) sulfur removal from the fuel gas with a zinc ferrite sorbent, with high efficiency cyclones and ceramic filters for particulate removal. Details of the performance and cost models for this system are reported elsewhere [3].

Two key design variables for the fixed bed zinc ferrite process are the sulfur absorption cycle time and the reactor vessel length-to-diameter ratio. The sulfur absorption cycle time is constrained to be at least as great as the time required to regenerate a bed of sulfated sorbent and return it to active service after a regeneration cycle. As the sulfur absorption time becomes longer, more sorbent is required to capture the syngas sulfur species over the increased time period. Larger absorption cycle times therefore require either larger reactor vessels and/or more reactor vessels, which increases the cost. The length-to-diameter ratio of the reactor vessel also affects process economics.

Another key area of uncertainty for this technology is the  $\text{NO}_x$  emission rate. Thermal  $\text{NO}_x$  emissions are expected to be quite low for IGCC systems due to the low heating value of the fuel gas and the presence of thermal diluents such as  $\text{H}_2\text{O}$ ,  $\text{CO}_2$  and  $\text{N}_2$  [15]. However, the hot gas cleanup system employed by the air-blown Lurgi system does not remove fuel-bound nitrogen (in the form of ammonia) from the fuel gas, and a substantial portion of the ammonia is converted to  $\text{NO}_x$  upon combustion. Thus,  $\text{NO}_x$  emissions pose a critical concern for systems with hot gas cleanup. For example, using conventional combustors the USDOE performance model of the Lurgi-based IGCC system yields  $\text{NO}_x$  emissions nearly four times greater than U.S. federal new source performance standard (NSPS) of 260 ng/J (0.6 lbs/10<sup>6</sup> Btu) for coal-fired power plants.

Future levels of NO<sub>x</sub> emissions are likely to be subject to much more stringent requirements because of the role of NO<sub>x</sub> in acid rain and tropospheric ozone formation.

To mitigate NO<sub>x</sub> emissions, several approaches are possible. In the near term, the most likely approach is the use of post-combustion exhaust gas NO<sub>x</sub> reduction technology. In the longer term, advanced staged combustion designs featuring rich/lean combustion may be commercialized and employed for fuels with high nitrogen content. In this study, we consider the use of selective catalytic reduction (SCR) for NO<sub>x</sub> control. In a SCR system, ammonia is injected into the flue gas upstream of a catalytic reactor through a set of nozzles comprising an injection grid. Because of the temperature window required for typical SCR catalysts, the SCR reactor employed with gas turbine combined cycle systems is typically located in the heat recovery steam generator. We employ a new performance and cost model of an SCR system [16] to explore the effects of two key design variables: the required NO<sub>x</sub> removal efficiency, which has a substantial impact on the catalyst volume requirement, and the catalyst layer replacement interval, which can be varied to achieve trade-offs between initial capital cost and annual replacement costs for catalyst. Since the cost of catalyst is a major expense for SCR systems, optimizing this process design is of significant interest.

Key performance and cost parameters of the engineering models for the IGCC system were assigned probability distributions based on data analysis, literature review, and the elicitation of expert judgments. The characterization of performance uncertainties focused on four major process areas: gasification, zinc ferrite desulfurization, gas turbine, and the SCR unit. Uncertainties in additional cost model parameters also were characterized, including direct and indirect capital

Table 1. Uncertain model parameters for illustrative case studies

Description and units <sup>a</sup>	Det. Val <sup>b</sup>	Type	Min	Max	Other
Gasifier fines carryover, wt-% of coal feed	5.0	F	0.0	1.0	5%
			1.0	3.5	20%
			3.5	5.0	25%
			5.0	8.0	25%
			8.0	15.0	15%
Fines capture in recycle cyclone wt-% of fines carryover	95	F	15.0	20.0	5%
			20.0	30.0	5%
			50	90	25%
			90	95	25%
			95	97	25%
Carbon retention in the bottom ash, wt-%	2.5	T	0.75	10.0	2.5
Gasifier coal throughput, lb DAF coal/(h-ft <sup>2</sup> )	305	T	152	381	305
Gasifier NH <sub>3</sub> yield, % of coal-N converted	0.9	T	0.5	1.0	0.9
Gasifier air/coal ratio, lb air/lb DAF coal	3.1	T	2.7	3.4	3.1
Steam/coal ratio, lb steam/lb DAF coal					
air/coal = 2.7	0.81	U	0.54	1.08	—
air/coal = 3.1	1.55	U	1.24	1.86	—
air/coal = 3.4	2.38	U	2.04	2.72	—
Zinc ferrite sorbent sulfur loading, wt-% sulfur in sorbent	17.0	N	2.16	31.84	17.0
Zinc ferrite sorbent attrition rate, wt-% sorbent loss per absorption cycle	1.0	F	0.17	0.34	5%
			0.34	0.50	20%
			0.50	1.10	25%
			1.10	1.50	25%
			1.50	5.00	20%
			5.00	25.00	5%
Fuel NO <sub>x</sub> , % conversion of NH <sub>3</sub> to NO <sub>x</sub>	90	T	50	100	90
Gasifier direct cost uncertainty, % of estimated direct capital cost	20	U	10	30	—
Sulfuric acid direct cost uncertainty, % of estimated direct capital cost	10	U	0	20	—
Gas turbine direct cost uncertainty, % of estimated direct capital cost	25	U	0	50	—
SCR unit catalyst cost, \$/ft <sup>3</sup>	840	U	250	840	—
Standard error of HRSG direct cost model, \$Million	0	N	-17.3	17.3	—
Maintenance cost factor, gasification, % of process area total cost	3	T	2	12	3
Maintenance cost factor, combined cycle, % of process area total cost	2	T	1.5	6	2
Unit cost of zinc ferrite sorbent, \$/lb	3.00	T	0.75	5.00	3.00
Indirect construction cost factor, %	20	T	15	25	20
Project contingency factor, %	17.5	U	10	25	—

<sup>a</sup>DAF = dry, ash free; SCR = selective catalytic reduction; HRSG = heat recovery steam generator. <sup>b</sup>Det. Val. = deterministic (point-estimate) value; min/max ( $\pm 3\sigma$  for N); and mode (T) or prob (F). Next columns indicate type of distribution (F = fractile, T = triangular, N = normal, U = uniform).

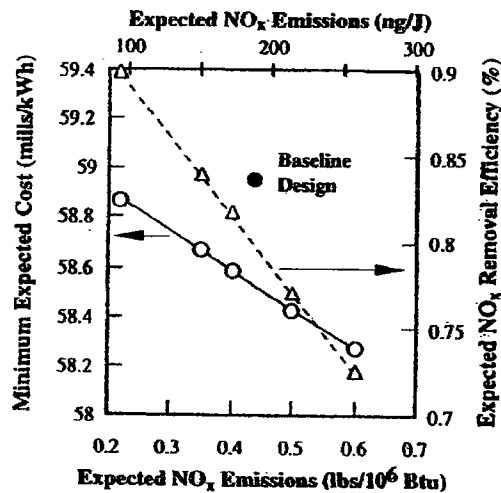


Fig. 5. Minimization of total levelized cost subject to expected value.

costs, operating and maintenance costs, financial assumptions, and the unit costs of consumables, byproducts, and wastes. Through an interactive screening process, the initial set of approximately 50 uncertain variables was narrowed to a set of 20 which most significantly affected uncertainty in plant efficiency, emissions, capital cost, and total levelized cost. These variables are listed in Table 1.

Figures 5–7 show the results of different stochastic optimization and stochastic programming problems applied to the IGCC flowsheet. Figure 5 first shows results of a stochastic optimization problem in which the expected cost of electricity (COE) is minimized for different levels of  $\text{NO}_x$  control (note that mills/kWh is identical to dollars/MWh). As the expected (mean) value of  $\text{NO}_x$  emissions is decreased, the expected value of  $\text{NO}_x$  removal efficiency in the SCR unit increases proportionally. The cost of the optimal design also increases as emissions decrease. As seen in Fig. 5, the optimal design reduces the expected COE by 0.5 mills/kWh relative to the base case design achieving 190 ng/J (0.44 lbs  $\text{NO}_x$ /10<sup>6</sup> Btu). For the 650 MW plant modeled in this example, this is equivalent to a total savings of approximately \$2 million per year. This savings is a measure of the benefit resulting from use of the new stochastic method to optimize the design parameters of the zinc ferrite and SCR units.

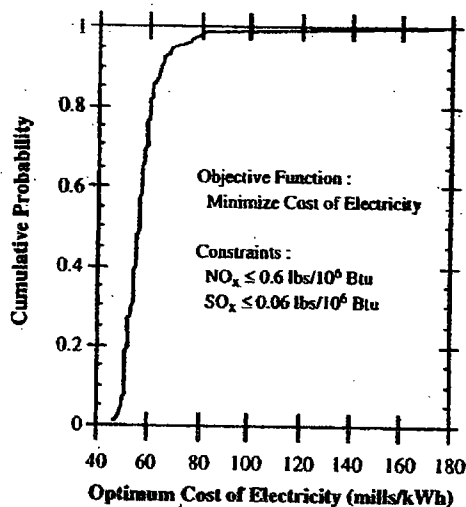


Fig. 6. Effect of uncertainties on minimum cost of the Lurgi IGCC system.

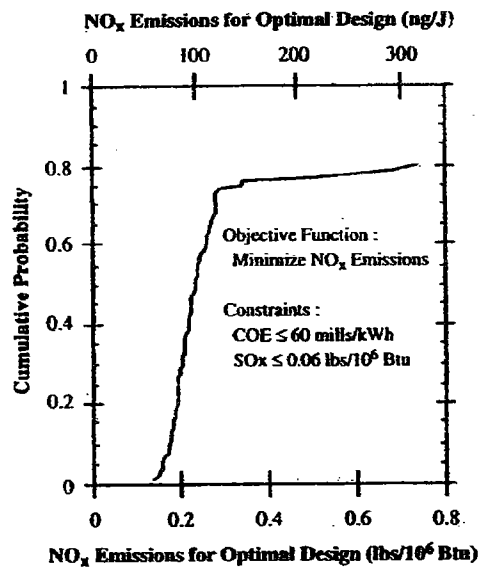


Fig. 7. Effect of uncertainties on minimum  $\text{NO}_x$  emissions for a given cost constraint.

Figure 5 also shows that the expected cost of the optimal design increases by 0.6 mills/kWh as  $\text{NO}_x$  is lowered from 260 to 95 ng/J (0.6 to 0.22 lbs/ $10^6$  Btu). This provides an indication of the expected cost impact of a three-fold tightening of current U.S. standards. Over this range, the optimal SCR removal efficiency increases from 73 to 90%, the latter being the maximum value established by the performance model.

To illustrate results for a stochastic programming formulation, Figure 6 next shows the effect of uncertainties on the cost of an optimal design. Here,  $\text{NO}_x$  emissions are constrained to 215 ng/J (0.5 lbs/ $10^6$  Btu) or less, and  $\text{SO}_2$  emissions 26 ng/J (to 0.06 lbs/ $10^6$  Btu) or less (the USDOE design goal of one tenth the current U.S. federal standard). A cumulative distribution function (CDF) is generated for a sample size of 100 iterations. The cost of electricity for the optimal design configuration is seen to vary by more than a factor of four due to the performance and cost uncertainties in the variables shown in Table 1. An 80% confidence interval gives expected costs between 45.0 and 60.0 mills/kWh.

Figure 7 shows another example in which  $\text{NO}_x$  emissions are minimized subject to a constraint of 60 mills/kWh on the maximum cost of electricity, representing an assumed upper bound on economic risk. The stochastic programming results for this case show a 45% probability of optimal designs achieving between 86 and 130 ng/J (0.2 and 0.3 lbs  $\text{NO}_x$ / $10^6$  Btu). The median value of the probabilistic results shows a  $\text{NO}_x$  emission rate of 104 ng/J (0.24 lbs/ $10^6$  Btu) for this case. Figure 7 also shows a 20% chance of being unable to meet the cost constraint, 2% of these designs have  $\text{NO}_x$  emissions exceeding 260 ng/J (0.6 lbs/ $10^6$  Btu), which is the Federal New Source Performance Standard for coal-fired power plants. For these cases, there is a significant risk that the process may not be viable under the economic constraints imposed in this example, since the plant might not comply with applicable emission limits.

These results are intended only to be illustrative of the new modeling capabilities now possible with stochastic optimization and stochastic programming. Additional case studies for other advanced power systems, including other IGCC designs, pressurized fluid bed combustion (PFBC) systems, and externally fired combined cycle (EFCC) systems currently are in progress. In conjunction with these efforts, on-going work also is developing new or improved cost and performance models for selected process components and systems for IGCC, PFBC and EFCC designs. These new models will form the basis for systematic comparisons of alternative coal-based power systems, and the effects of uncertainties on their optimal design, cost and performance.

## CONCLUSIONS

This paper has described a set of new systems analysis tools and methods that can substantially improve the design and analysis of advanced coal-based energy systems. By enhancing existing process simulators with the mathematical methods presented here (i.e. probabilistic modeling, optimization, and MINLP synthesis), researchers and research managers now can tackle a wide range of system performance and cost analysis not heretofore possible. This new toolbox can be used in conjunction with new or existing process performance and cost models to insure that process design issues are more fully and rigorously considered in all phases of activity. These modeling tools also can be extended to a host of other technology applications where process design, cost minimization, risk analysis, environmental compliance and R&D prioritization remain important issue.

*Acknowledgements*—This work was supported under Contract no. DE-AC21-92MC29094 from the U.S. Department of Energy, Morgantown Energy Technology Center.

## REFERENCES

1. Diwekar, U. M. and Rubin, E. S., *Computers and Chemical Engineering*, 1991, **15**, 105.
2. Massachusetts Institute of Technology, ASPEN User's Manual, Vol. 1. Reports DOE/MC/16481-1203. NTIS/DE82020196, 1982.
3. Frey, H. C. and Rubin, E. S., *I & EC Research*, 1992a, **31**, 1299.
4. Frey, H. C. and Rubin, E. S., *Environmental Science Technology*, 1992b, **26**.
5. Frey, H. C., Rubin, E. S. and Diwekar, U. M., *Energy*, 1994, **19**(4), 449.
6. Gill, P. E., Murray, W. and Wright, M. H., *Practical Optimization*. Academic Press, London, 1981.
7. Biegler, L. T., *Proceedings of the 2nd International Conference on Foundations of Computer Aided Process Design*, 1983.
8. Biegler, L. T. and Cuthrell, J. E., *Computers and Chemical Engineering*, 1985, **9**, 257-271.
9. Diwekar, U. M., Frey, H. C. and Rubin, E. S., *I & EC Research*, 1992, **31**, 1927.
10. Diwekar, U. M., Grossman, I. E. and Rubin, E. S., *I & EC Research*, 1991, **31**, 313.
11. Marsten, R., User's Manual for ZOOM/XMP, The Department of Management Information Systems, University of Arizona, Tucson, 1986.
12. Lang, Y. D. and Biegler, L. T., *Computers and Chemical Engineering*, 1987, **11**, 143.
13. Kravanja, Z. and Grossman, I. E., *Computers and Chemical Engineering*, 1990, **14**, 1363.
14. Diwekar, U. M. and Rubin, E. S., *I & EC Research*, 1993, **32**, 2006-2011.
15. Holt, N. A., Clark, E. and Cohn, A., *Symposium on Stationary Combustion Nitrogen Oxide Control*, Vol. 1, GS-6453. Electric Power Research Institute, Palo Alto, CA, July, 5A-17, 1989.
16. Frey, H. C., Performance Models of Selective Catalytic Reduction NO<sub>x</sub> Control Systems, Quarterly report from Carnegie Mellon University to U.S. Department of Energy, Pittsburgh, PA 15213, 1993.
17. Diwekar, U. M. and Rubin, E. S., *I & EC Research*, 1994, **33**, 292.